QFT AUTOPILOT DESIGN FOR ROBUST CONTROL OF SHIP COURSE-KEEPING AND COURSE-CHANGING PROBLEMS

Viorel Nicolau[*], Constantin Miholcă[*], Dorel Aiordachioaie[*] and Emil Ceangă[**]

[*]*Department of Electronics and Telecommunications, "Dunărea de Jos" University of Galați, Faculty of Electrical Engineering, 47 Domneasca Street, Galati, 800008, Romania, e-mail: Viorel.Nicolau@ugal.ro, Constantin.Miholca@ugal.ro, Dorel.Aiordachioaie@ugal.ro*

[**]*Research Center in Advanced Process Control Systems, "Dunărea de Jos" University of Galați, Faculty of Electrical Engineering, 47 Domneasca Street, Galati, 800008, Romania, e-mail: Emil.Ceanga@ugal.ro*

Abstract: *This paper describes the design steps of robust QFT autopilot for the course-keeping and course-changing control of a ship, in the presence of disturbances. The ship model has parametric uncertainties, caused by the variations of hydrodynamic coefficients with the speed of the ship. Knowing the variation ranges of the model parameters, the QFT method (Quantitative Feedback Theory) can be used to design the ship autopilot with certain performance specifications. The autopilot must satisfy the robust stability, tracking performance and disturbance rejection conditions, for all ship models generated by the parameter variations within the uncertainty ranges.*

Keywords: *robust autopilot, QFT control, course-keeping, course-changing, Nomoto ship model.*

1. INTRODUCTION

Automatic control strategies for marine vehicles are in general designed to improve their functions with adequate reliability and economy. The main purpose of the rudder is to control the heading of the ship in course-keeping and course-changing maneuvers [1]. Applying more sophisticated autopilots for ship steering is mainly due to performance improvement and fuel economy [2].

A ship in waves is considered as a rigid body with six degrees of freedom. Nonlinear mathematical models of ship dynamics are used for simulation of ship motions and for design of the closed loop control systems. Model structure and parameter values can be estimated in model basin test, but full-scale verifications are also required [3].

Taking into account only yaw motion of the ship, the steering dynamics can be described by simple linear [4] or nonlinear [5] transfer functions. In this case, the heading control systems (also called autopilot systems) are of monovariable type. Their main purpose is to command the steering machine, moving the

rudder, so that the ship to track a desired route, which can be specified by way-points [1].

Ship steering control systems are designed to perform two entirely different functions: course-keeping and course-changing maneuvers [6].

In the first case, the autopilot acts to maintain the ship on a set course (between any two adjacent way-points) in the presence of disturbances. This type of system is fully autonomous in that it does not need an operator to provide commands during operation.

In the second case, the autopilot provides good manoeuvrability, changing the ship course to a new way-point, in accordance with commanded course changes given by the superior control level or pilot/helmsman. In general, the yaw angle changes are small enough so the linear ship models can be used. However, for large maneuvers, the nonlinear ship models must be taken into account.

Conventional ship autopilot for course-keeping and course-changing control problems involves the heading angle feedback, as shown in Fig. 1. The yaw motion of the ship is described by the transfer function $H_S(s)$ from the rudder angle (δ) to the course angle (ψ). The autopilot generates the rudder commands, based on the course error (ψ_e), which appears due to external disturbances.

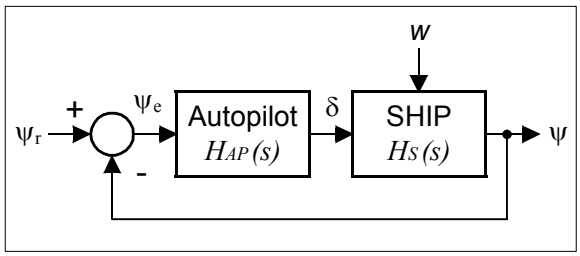

Fig. 1. Autopilot closed loop for heading control systems

The external disturbances are generated by environmental conditions (e.g. first and second order waves, wind, marine currents) or by control systems (e.g. steering system, propulsion system). The waves are the most important external disturbances and they are considered in this paper.

In addition, the operational conditions (e.g. trim, load or ballast condition, speed changes, water depth) affect the ship dynamics, modifying the hydrodynamic coefficients of the ship and the corresponding parameters of ship model.

If the mathematical model of the controlled physical process presents parametric uncertainties, it is necessary to use robust control techniques for controller design. Since the model parameters of the ship's yaw motion depend on the forward speed as well as the weather conditions, the ship model presents parametric uncertainties.

Therefore, robust control theory should be considered, like H-inf theory [7], [8], [9], sliding mode control [10], QFT method [11], [12], neural networks [13] etc.

In H-inf theory, desired properties for the closed-loop transfer function are embodied into weighting operators that shape output and control signals [14]. Selecting the weighting operators assures robust performances, but this is a difficult task. The H-inf approach is frequently used, especially for nonparametric uncertainties.

In practice, the forward speed of the ship affects the ship dynamics, and the speed value is chosen by economical criteria, like fuel consumption, navigation safety, voyage period. For the heading control problems, the influence of the forward speed on the ship model parameters is very important. Also, the ascertainment of the model parameter variation range into usual limits of the forward speed is not a difficult problem, which can be done by experiments with a ship model or with the ship in open sea.

It is desired to use a direct way for the autopilot design without explicitly solving the underlying H-inf problem. Therefore, the QFT method has been chosen for the autopilot design. In addition, the method permits that the structure of autopilot to be determined up-front.

The goal of this paper is to design robust QFT autopilot for course-keeping and course-changing control of a ship, in the presence of disturbances.

The course-keeping autopilot takes into account the wave influence on the yaw motion, corrected with the ship's speed and the incidence angle [15]. Robust stability and input disturbance rejection conditions are specified, to meet the course-keeping requirements in the presence of the first order wave disturbances.

The course-changing autopilot satisfies some performance specifications, like robust stability and tracking performance conditions, in a similar manner as in [11]. In addition, input disturbance rejection conditions are imposed and

bigger uncertainty ranges of the ship parameters are considered [16].

The paper is organized as follows. Section2 provides mathematical models used in simulations. In section 3, the algorithm of QFT method is presented. In section 4, performance specifications are generated for both course-keeping and course-changing autopilots. Section 5 describes the design steps for robust QFT autopilot and simulation results which are obtained for some numerical examples. Conclusions are presented in section 6.

2. MATHEMATICAL MODELS

As a requisite for the simulation results, models of ship dynamics and wave disturbances had to be generated.

2.1 *Ship Dynamics*

The equations describing the horizontal motion of a ship are derived by using Newton's laws, expressing conservation of hydrodynamic forces and moments. Then, the model can be simplified applying Taylor series for hydrodynamic forces and moments [17]. A three degree-of-freedom linear model is obtained for asymmetric ship motions, with coupled sway-yaw-roll equations, which can be identified.

Using the Laplace transform and eliminating the sway speed (v), two transfer functions result ($H_{\delta\psi}$ and $H_{\delta\varphi}$) which describe the transfer from rudder angle (δ) to yaw angle (ψ) and to roll angle (φ) respectively.

The responses of the ship to the external disturbances are usually computed by applying the principle of superposition.

Considering only first order wave disturbances (w), the Laplace equations for linear ship model are [18]:

$$\begin{cases} \psi(s) = H_{\delta\psi}(s) \cdot \delta(s) + H_{w\psi}(s) \cdot w(s) \\ \varphi(s) = H_{\delta\varphi}(s) \cdot \delta(s) + H_{w\varphi}(s) \cdot w(s) \end{cases} \quad (1)$$

The transfer functions have parameters depending on the speed of the ship (u) and the incidence angle (γ), which is the angle between the heading and the main direction of the wave. It should be noted that the linear model is not valid for large maneuvers, and the nonlinear ship models must be taken into account [19].

The first Laplace equation in (1) describes the yaw angle dependencies of the rudder angle and wave perturbation. The wave influence on the yaw motion represents the hydrodynamic moment of rotation around Oz axis (N_w), which is generated by waves.

Considering the linear model of the ship, the additive disturbances can be moved at the system input. Therefore, the wave perturbation is treated as input noise (p) for the ship model, so that the Laplace equation for yaw motion can be written:

$$\psi(s) = H_{\delta\psi}(s) \cdot \delta(s) + H_{\delta\psi}(s) \cdot p(s) \quad (2)$$

The transfer function $H_{\delta\psi}$ represents the ship model with uncertainties, due to the hydrodynamic coefficients, which depend on operating conditions of the vessel.

The monovariabile linear model of the ship's dynamics for yaw motion, without considering any perturbations, can be represented as a first order Nomoto model [4], whose differential equation is:

$$\ddot{\psi}(t) + \frac{1}{T} \cdot \dot{\psi}(t) = \frac{k}{T} \cdot \delta(t) \quad (3)$$

The corresponding transfer function is:

$$H_{\delta\psi}(s) = \frac{\psi(s)}{\delta(s)} = \frac{k}{s(Ts+1)}, \quad (4)$$

where the parameters k and T depend on the operating conditions such as ship's speed, load or ballast situation, water depth etc.

The Nomoto model provides a reasonably accurate representation, if the rudder angles are relatively small. This is the case for course-keeping control and for slight course changes.

Also, the model can be used for course-changing problem, if the way-points of the desired route are computed and generated so that smooth rudder angles are obtained.

When important course changes are needed, the rudder angles are big and a nonlinear term must be added to Nomoto equation, resulting the Norrbin model [5]:

$$T\dot{r} + H_N(r) = k \cdot \delta, \quad (5)$$

where

$$r = \dot{\psi} \quad \text{and} \quad H_N(r) = n_3 r^3 + n_2 r^2 + n_1 r + n_0 \quad (6)$$

The vessel particularities define the values of Norrbin coefficients. For course stabile ships

with lateral symmetry ($n_2=n_0=0$ and $n_1=1$), the Norrbin model is:

$$\ddot{\psi}(t) + \frac{1}{T}\cdot\dot{\psi}(t) + \frac{1}{T}\cdot n_3\cdot\dot{\psi}^3(t) = \frac{k}{T}\cdot\delta(t) \qquad (7)$$

In this paper, Nomoto model in (4) is used. The model parameters depend on the ship's speed and this dependency is identified in [18].

2.2. *Wave Model*

The generation of the waves is rather complex. Irregular waves can be modeled taking into account their stochastic nature. In this case, the wave can be regarded as an ergodic random process with elevation $\zeta(t)$ and zero mean. Knowing the mean square spectral density function $\phi_{\zeta\zeta}(\omega)$ of the wave elevation $\zeta(t)$, shortly called wave spectrum, the statistical parameters of the wave can be computed and the wave model can be generated [20].

Based on the wave spectrum, the wave disturbance can be modeled as the sum of a limited number of sinusoidal waves with different amplitudes, frequencies and phase angles:

$$w(t) = \sum_{i=1}^{N} A_i \cdot \sin(\omega_i \cdot t + \varphi_i) \qquad (8)$$

where A_i and ω_i are the amplitude and angular frequency of the i-th component, and φ_i is the phase angle randomly drawn from a uniform density distribution.

Considering the discrete wave spectrum, the amplitude A_i is [20]:

$$A_i = \sqrt{2\cdot\phi_{\zeta\zeta}(\omega_i)\cdot\Delta\omega} \qquad (9)$$

where $\Delta\omega$ represents the discrete frequency step, which is imposed.

The relative frequency between the wave and the ship modifies the wave spectrum and this transformation must be taken into account for wave model generation [15].

3. QFT METHOD

The QFT method is a robust design technique for the linear or nonlinear systems with parametric uncertainties, which are affected by external disturbances.

It is a frequency domain technique, using the Nichols chart to achieve the desired performance specifications of the close-loop system, over the specified region of parameter uncertainties [12].

If the system is nonlinear, the method can be used with equivalent linear system, but the variation intervals of system parameters must be wide enough to include the nonlinear behavior.

The autopilot design by QFT method considers the Nomoto model of the ship like a system with parametric uncertainties, affected by external perturbations (p).

The closed loop and the general autopilot structure are illustrated in Fig. 2. The autopilot has two linear components: the compensator $G(s)$ and the prefilter $F(s)$.

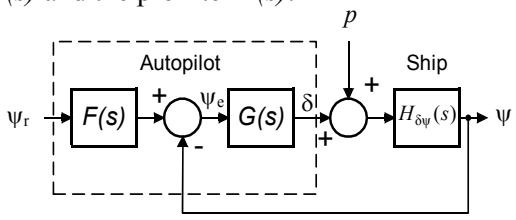

Fig. 2. QFT autopilot structure

The goal is to design the autopilot so that the closed loop system to fulfill the robust stability, input disturbance rejection and tracking specifications, with specific values for course-keeping and course-changing problems.

4. DESIGN SPECIFICATIONS

The hydrodynamic characteristics of the ship depend on the forward speed. This dependency was identified in [18], for a frigate class ship and four different ship's speed: 10, 14, 18 and 22 knots.

The frequency characteristics of the ship model are different with the speed, as shown in Fig. 3.

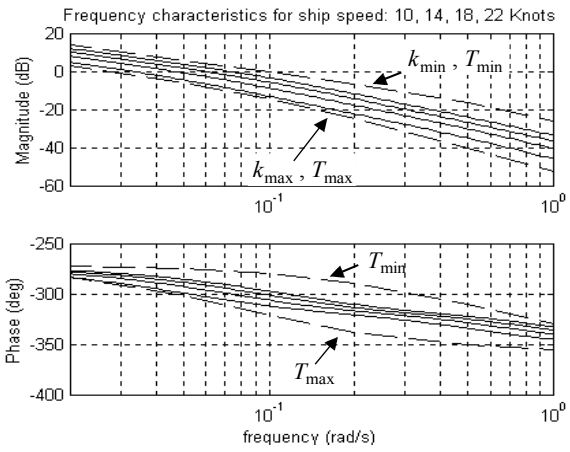

Fig. 3. Frequency characteristics of the ship model

4.1. *Uncertainty Region of the Ship Model*

The two parameters of the Nomoto model (k and T) have variations with the ship speed, in two value ranges:

$$[k_{min}, k_{max}] \text{ and } [T_{min}, T_{max}] \quad (10)$$

These variations modify the frequency characteristics of the ship model.

The goal is to specify the value intervals of model parameters, so that the frequency characteristics to be within the limits for all values of the speed.

The four frequency characteristics, illustrated with continuous lines in Fig.3, are included in two limit characteristics, which are represented with dashed lines. These limits correspond to Nomoto models generated by:

$$k \in [-0.1, -0.03] \text{ and } T \in [1.7, 12] \quad (11)$$

As a result, an uncertainty region appears, generated by the value ranges of ship parameters. This region is illustrated in Fig.4.

If the performance specifications are met for the plant models placed on the contour of uncertainty region, then they are met for all plant models into the region. Therefore, only a small number (N) of models on the contour must be selected for QFT design.

In this paper, six equidistant values are considered for the two parameters of the ship model (k and T), resulting 20 different ship models on the contour (N = 20), which are marked distinctly in figures 4 and 5.

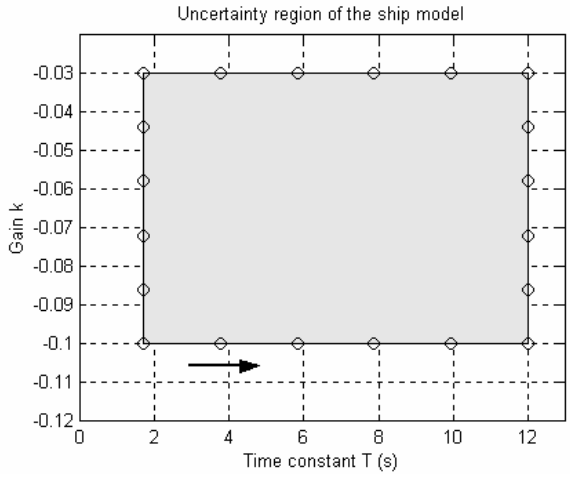

Fig. 4. Uncertainty region generated by parameter values

For every frequency value, the characteristics of all ship models (generated by uncertainty region) represent points of a template, which is a closed contour into Nichols chart.

For example, the template of ship models generated for the frequency ω = 0.1 rad/s is represented in Fig. 5.

The boundary of the template can be obtained by mapping the boundary of the uncertainty region. Templates for other values of frequency are obtained in a similar manner.

The corresponding points on both contours in Fig. 4 and Fig. 5 respectively can be found by crossing the contours in the ways indicated by arrows.

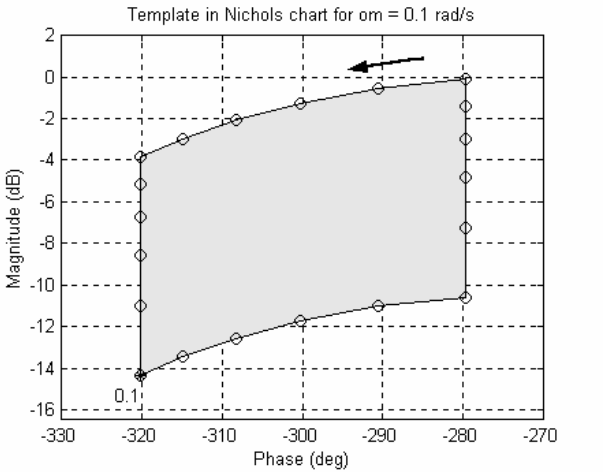

Fig. 5. Template of ship models in Nichols chart

The lower-left corner into the uncertainty region corresponds to the upper-right corner of the template.

4.2. *Stability Specifications*

The stability specifications assure the stability of the closed loop system for all possible variations of the model parameters into the uncertainty region.

The closed loop transfer function is:

$$H_B(s) = \frac{G(s) \cdot H_{\delta\psi}(s)}{1 + G(s) \cdot H_{\delta\psi}(s)} = \frac{L(s)}{1 + L(s)}, \quad (12)$$

where $L(s)$ represents the loop transmission function.

For every frequency into the working bandwidth, the envelope of the magnitude characteristics must be smaller than a maximum value α_B:

$$\max_{H_{\delta\psi}(s),\, \omega} \left(\left| H_B(j\omega) \right| \right) \le \alpha_B, \quad (13)$$

where in general $\alpha_B < 2$ dB. The chosen value is $\alpha_B = 1.2 \cong 1.6$ dB. The stability specifications must be met by both types of autopilot.

4.3. *Robust Tracking Specifications*

The course changes must be defined within acceptable range of variations. When a course change is commanded, the reference course followed by the vessel can be specified by means of a second order reference model:

$$H_0(s) = \frac{\omega_0^2}{s^2 + 2\zeta\omega_0 s + \omega_0^2}, \tag{14}$$

where ω_0 is the natural frequency and ζ is the damping coefficient of the closed loop reference model.

For course-changing without oscillations, the damping coefficient is recommended to be [1]:

$$\zeta \in [0.8, 1].$$

In this paper, the selected values are: $\omega_0 = 0.1$ rad/s and $\zeta = 0.9$.

The closed loop tracking system has the transfer function:

$$H_T(s) = \frac{F(s)\cdot G(s)\cdot H_{\delta\psi}(s)}{1 + G(s)\cdot H_{\delta\psi}(s)} = \frac{F(s)\cdot L(s)}{1 + L(s)}, \tag{15}$$

which must be the same as H_0.

Due to parameter variations of the ship model, the closed loop system has also variations, which must remain within specific limits. These limits are defined by two transfer functions, denoted lower bound ($H_{0L}(s)$) and upper bound ($H_{0U}(s)$) respectively.

The magnitude characteristics satisfy the inequalities:

$$\left|H_{0L}(j\omega)\right| \le \left|H_T(j\omega)\right| \le \left|H_{0U}(j\omega)\right| \tag{16}$$

The two transfer functions represent robust tracking tolerances and must include the reference model H_0:

$$\left|H_{0L}(j\omega)\right| \le \left|H_0(j\omega)\right| \le \left|H_{0U}(j\omega)\right| \tag{17}$$

Hence, the lower- and upper-limit transfer functions are selected around the second order reference model:

$$H_{0L}(s) = \frac{a_1 \cdot a_2 \cdot a_3}{(s + a_1)(s + a_2)(s + a_3)} \tag{18}$$

$$H_{0U}(s) = \frac{\frac{\omega_0^2}{a}(s + a)}{s^2 + 2\zeta\omega_0 s + \omega_0^2}, \tag{19}$$

where the parameter values are: $a_1 = 0.5\cdot\omega_0$, $a_2 = 1.5\cdot\omega_0$, $a_3 = 2\cdot\omega_0$ and $a = 1.2\cdot\omega_0$.

The magnitude characteristics of the desired second order reference model and lower- and upper-limit transfer functions are illustrated in Fig. 6.

It can be observed that the ship dynamics of the yaw motion are important for very low frequencies and they decrease rapidly for frequencies bigger than $\omega_0 = 0.1$ rad/s.

The step responses of the transfer functions defined in (14), (18) and (19) are represented in Fig. 7. The course changes last tens of seconds and depend on the operational conditions.

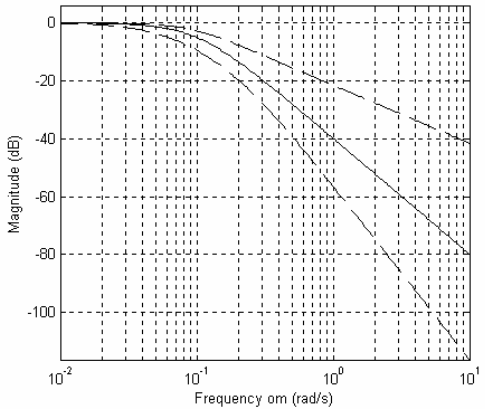

Fig. 6. Magnitude characteristics of the reference and tracking bound models

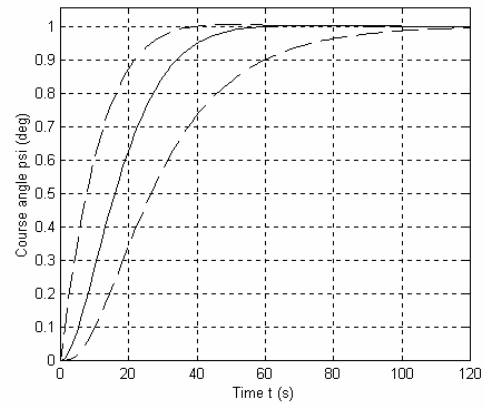

Fig. 7. Step responses of the reference and tracking bound models

The continuous lines correspond to the reference model and the dashed lines illustrate the tracking tolerances of the lower and upper bounds.

4.4. *Input Disturbance Rejection Specifications*

The input disturbance rejection specifications are defined for the transfer function:

$$H_P(s) = \frac{H_{\delta\psi}(s)}{1+G(s)\cdot H_{\delta\psi}(s)} = \frac{H_{\delta\psi}(s)}{1+L(s)} \quad (20)$$

For all possible variations of the model parameters into the uncertainty region, the magnitude characteristic envelope of the perturbation channel must be smaller than a maximum value α_P:

$$\max_{H_{\delta\psi}(s),\,\omega} \left(\left|H_P(j\omega)\right|\right) \le \alpha_P, \quad (21)$$

where the chosen value is $\alpha_P = 0.1 = -20$ dB.

4.5. *Ship model templates*

The goal of this step is to obtain ship model templates at specified frequencies that pictorially describe the region of plant parameter uncertainty on the Nichols chart. Then, the nominal ship model is chosen.

For every point of a chosen frequency vector into the system bandwidth, a ship model template is obtained in Nichols chart, by computing the frequency responses of all ship models (N = 20) selected on the contour of the uncertainty region.

The template shape depends on the frequency value. Starting from low frequencies, the template width increases, then as frequency takes on larger values, the templates become narrower, tending to a vertical line when the frequency tends to infinity.

In Fig. 8, six templates are represented, corresponding to six frequency values into the system bandwidth:

w_1 = 0.02, 0.05, 0.1, 0.2, 0.5 and 1 rad/s (22)

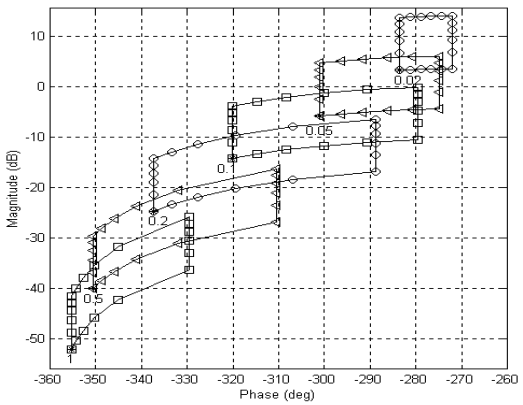

Fig. 8. Ship model templates for six frequency values

The frequency responses for all selected models are computed with the function *freqcp.m* from QFT Toolbox of Matlab.

The nominal ship model is the one whose template point is always at the lower left corner (marked distinctly in Fig. 8) for all frequencies for which the templates are obtained. For the selected templates, the nominal ship model is:

$$k = k_{\max},\ T = T_{\max},\ H_{\delta\psi 0}(s) = \frac{-0.03}{s\cdot(12s+1)} \quad (23)$$

5. DESIGN AND SIMULATION RESULTS

Once the performance specifications are imposed, the QFT autopilot can be designed for course-changing and course-keeping problems. Also, the resulting closed loop system can be verified and simulated in the presence of first order wave disturbances.

For course-changing autopilot, the compensator *G(s)* and prefilter *F(s)* must be designed, while for course-keeping control, only *G(s)* must be determined.

5.1. *Course-changing autopilot*

In this case, robust stability and tracking specifications are used, with disturbance rejection conditions.

Due to the prefilter *F(s)*, the autopilot acts like a *real-PD* controller on reference channel, which is sufficient if the course change commands are step type signals. Such autopilot assures zero stationary error for step reference input, but it can not compensate the stationary errors if the system is used to track a desired trajectory $\psi_r(t)$.

On perturbation channel, the *real-PD* autopilot can not eliminate the stationary errors generated by constant-value disturbances, which is not this case, because the prefilter has no influence on perturbation input.

In addition, constant or slow varying drift effect produced by wind or marine currents can be compensated by periodic course corrections. Therefore, constant disturbances can be ignored, but the trajectory of the ship is not optimally.

The bounds of robust stability, robust tracking and input disturbance rejection are calculated, on the basis of the performance specifications, ship templates and nominal ship model, using *sisobnds.m* function from QFT Toolbox of Matlab. These bounds are illustrated in Fig. 9.

The tracking bounds (thin lines, denoted with 7) and input disturbance rejection bounds (thick lines, denoted with 3) are open contours, being calculated for the four smallest frequency values:

$w_2 =$ 0.02, 0.05, 0.1 and 0.2 rad/s (24)

The closed contours represent the stability bounds for all six frequency values of vector w_1. Considering the open contours, the bound magnitude is bigger for smaller frequencies. Also, the disturbance rejection bounds are above the tracking ones for the same frequency.

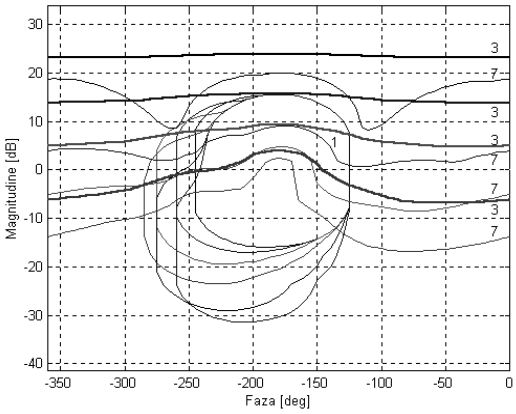

Fig. 9. Robust stability, tracking and disturbance rejection bounds

For every frequency value, the optimal bounds are calculated by intersecting all the bounds, as illustrated in Fig. 10, using *sectbnds.m* function from QFT Toolbox of Matlab.

On the same Nichols chart, the transfer function of the nominal loop transmission is represented (vertical line):

$$L_0(s) = G(s) \cdot H_{\delta\psi 0}(s), \tag{25}$$

where the initial expression of compensator *G(s)* can be chosen.

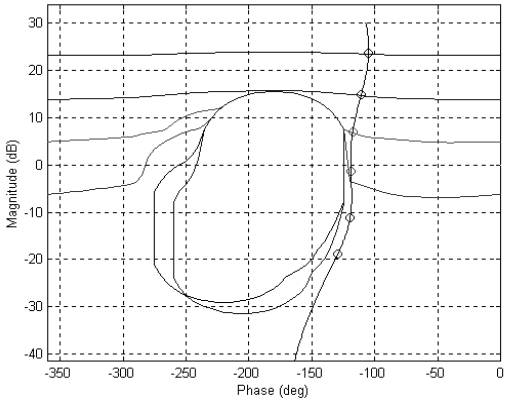

Fig. 10. Optimal bounds and nominal loop transmission for course-changing autopilot

The nominal loop transmission is calculated for an extended frequency vector, which includes the w_1 vector, with w_1 values marked distinctly in Fig. 10.

For this, the *lpshape.m* QFT function is used, which is a controller design environment for continuous-time linear systems. It produces the Nichols plot for the nominal loop transmission, while the compensator expression can be modified into an interactive manner.

In this way, modifying the compensator expression, the nominal loop transmission is synthesized to satisfy the optimal bounds, without penetrating the closed contours.

For every frequency value, the values of nominal loop transmission must be on or above the corresponding values of optimal bounds.

The final expression of the compensator, corresponding to the Nichols plot of the nominal loop transmission illustrated in Fig. 10, is:

$$G(s) = -\frac{83.5s^2 + 16.1s + 0.037}{s^2 + 1.53s} =$$

$$= \frac{-83.5 \cdot (s + 0.1905) \cdot (s + 0.002326)}{s \cdot (s + 1.53)} \tag{26}$$

It can be observed that the compensator is a *series-type PID* controller of the form:

$$G(s) = k_R \cdot \frac{T_I s + 1}{T_I s} \cdot \frac{T_D s + 1}{T_P s + 1}, \tag{27}$$

with parameter values:

$T_I = 430, \quad T_D = 5.25, \quad T_P = 0.6536$

and $k_R = -10.4$ (28)

The frequency characteristics of compensator G(s) are illustrated in Fig. 11.

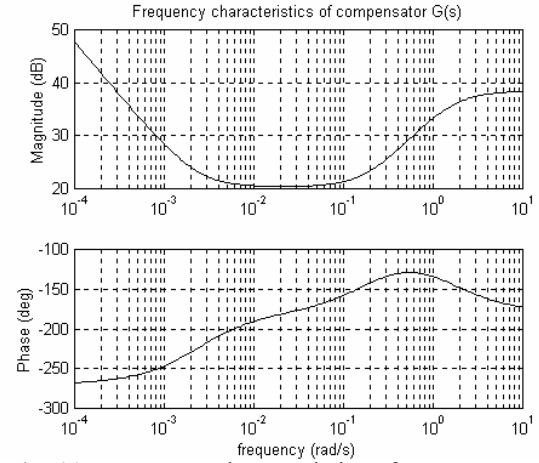

Fig. 11. Frequency characteristics of compensator G(s)

Big negative values of the phase are generated by negative value of gain k_R, which is caused by sign convention between rudder angle (positive to port side) and yaw angle movements (positive to starboard side).

The prefilter *F(s)* is synthesized to satisfy the tracking specifications, by modifying the expression interactively, starting from a structure determined up-front. The parameters of prefilter are modified, until the tracking specifications are met.

The final expression of prefilter is:

$$F(s) = \frac{0.058}{s + 0.058} \tag{29}$$

For robust tracking verification, the influence of the prefilter is illustrated in Fig. 12 and 13.

The upper and lower envelopes of magnitude characteristic variations of the closed loop system without prefilter are represented with continuous lines in Fig. 12. It can be observed that the envelopes are outside of the tracking limits (illustrated with dashed lines).

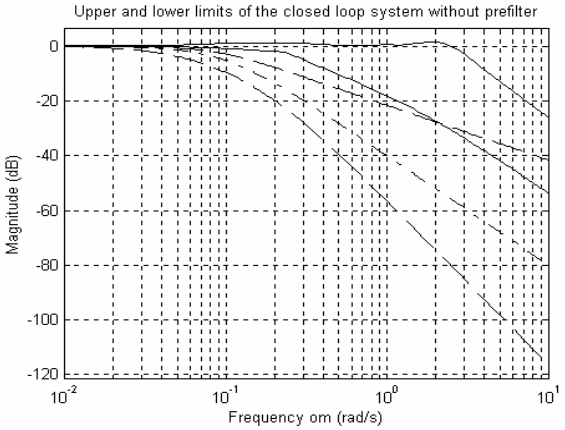

Fig. 12. Upper and lower magnitude envelopes of closed loop system without prefilter

Using the prefilter *F(s)*, the tracking specifications are satisfied, as shown in Fig. 13.

In this case, the upper and lower envelopes of the closed loop system with prefilter are inside of the tracking limits.

In figure, the magnitude characteristic of the reference model is also represented with dash-dot line.

The closed loop system verifies the robust stability specification, as shown in Fig. 14. The maximum value $\alpha_B = 1.2 \cong 1.6$ dB is represented with dashed line.

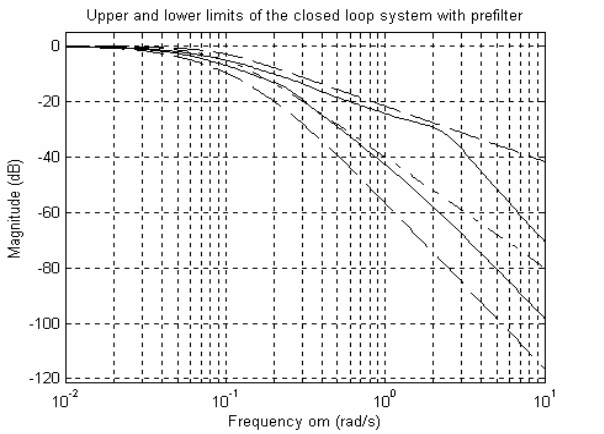

Fig. 13. Upper and lower magnitude envelopes of closed loop system with prefilter

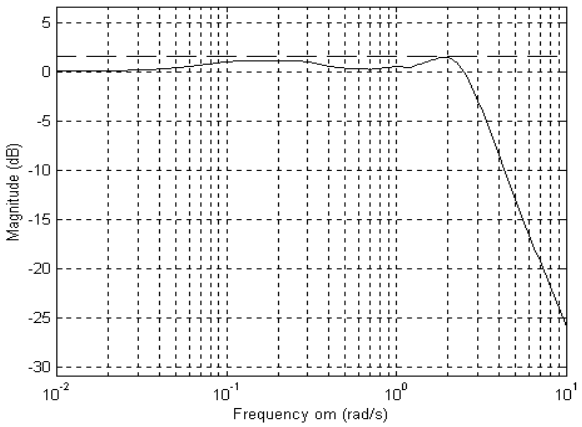

Fig. 14. Robust stability verification for course-changing autopilot

The maximum magnitude characteristic envelope is smaller than the specified value for the entire working bandwidth:

$$\max_{H_{\delta\psi}(s),\,\omega} \left(\left| H_B(j\omega) \right| \right) = 1.188 < \alpha_B = 1.2 \tag{30}$$

Also, the disturbance rejection condition is satisfied, as illustrated in Fig. 15.

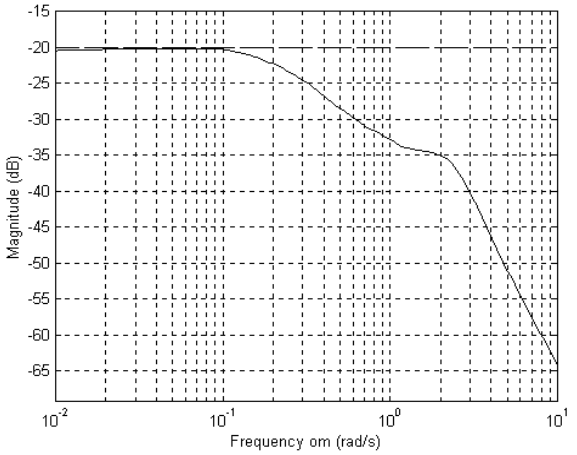

Fig. 15. Disturbance rejection verification

The maximum value $\alpha_P = 0.1 = -20$ dB is represented with dashed line.

The magnitude characteristic envelope of the perturbation channel is smaller than the specified value for the entire working bandwidth:

$$\max_{H_{\delta\psi}(s),\,\omega}\left(\left|H_P(j\omega)\right|\right) = 0.098 < \alpha_P = 0.1 \qquad (31)$$

The frequency characteristics of closed loop system for all N ship models on the contour of uncertainty region are illustrated in Fig. 16.

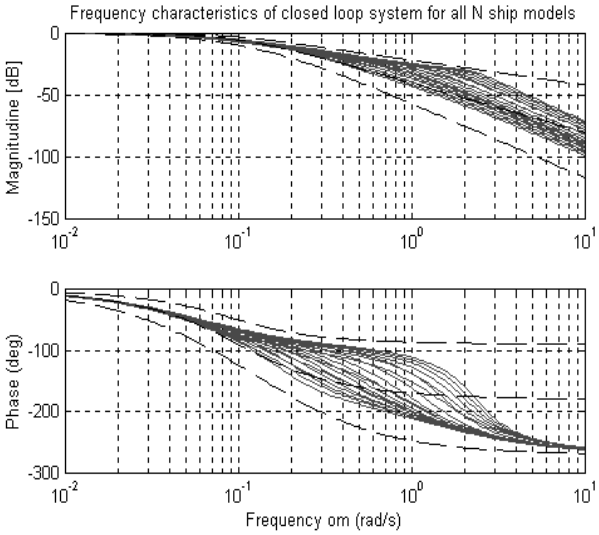

Fig. 16. Frequency characteristics of closed loop system for all N ship models on the contour

As expected, these characteristics are enclosed by upper and lower envelopes from Fig. 13. The reference model and tracking tolerances are represented with dashed lines.

The reference step responses of the closed loop system for all the ship models considered on the contour of the uncertainty region (N=20) are illustrated in Fig. 17. The course followed by the ship remains into the specified limits and approximates the second order reference model.

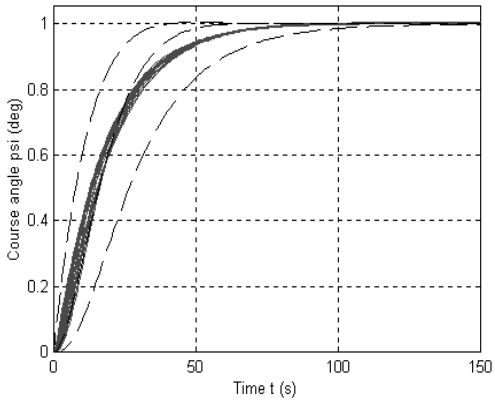

Fig. 17. Reference step responses of closed loop system for all N ship models on the contour

The step responses on perturbation channel of the closed loop system for all the ship models considered on the contour of the uncertainty region are illustrated in Fig. 18.

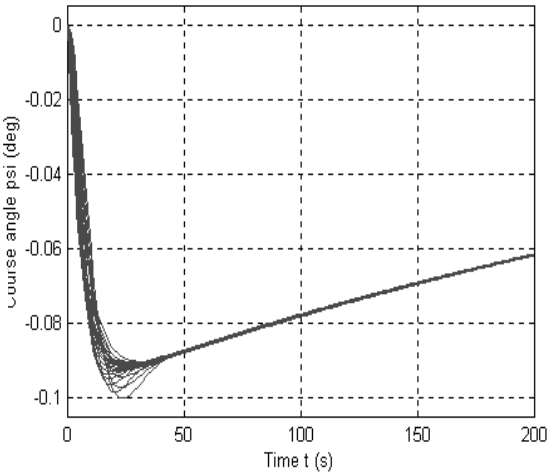

Fig. 18. Perturbation step responses of closed loop system for all N ship models on the contour

It can be observed that the disturbance rejection condition is satisfied for all ship models selected on the contour of the uncertainty region. Also, theoretically, the autopilot can compensate the constant-value disturbances, but the time constant is big.

To illustrate the course change in the presence of disturbances, a change command of 10 deg is considered simultaneously with wave disturbances.

The waves have the significant height $h_{1/3} = 4$ *m* and the incidence angle $\gamma = 135$ *deg*. The parameters of the ship model correspond to the ship speed $u = 22$ *Knots*.

The course-changing response of the ship is illustrated in Fig. 19. The tracking tolerances are represented with dashed lines.

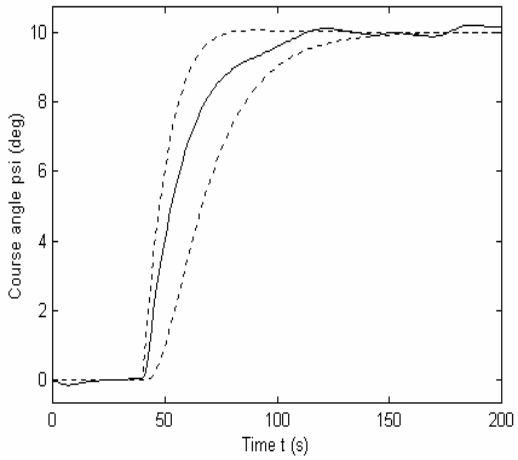

Fig. 19. Course-changing response of the ship in the presence of wave disturbances

The autopilot assures zero stationary error for step reference input, but it can not compensate the stationary errors if the system is used to track a desired trajectory $\psi_r(t)$. For example, a linear variable reference signal produces stationary error of the yaw angle, as illustrated in Fig. 20.

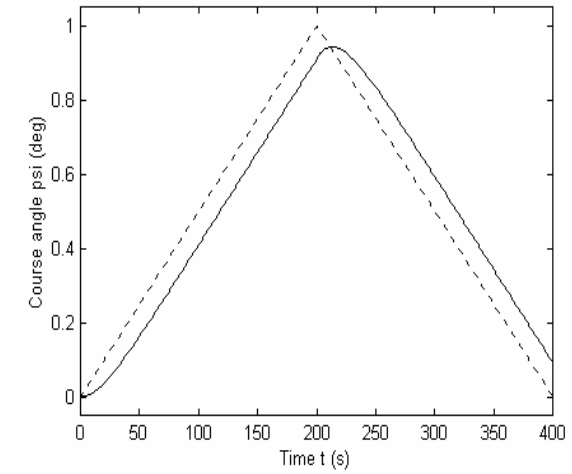

Fig. 20. Tracking errors of the yaw angle

In this case, the trajectory error is small and in addition, the errors can be compensated by periodic course corrections.

5.2. *Course-keeping autopilot*

For course-keeping problem, only the robust stability and disturbance rejection conditions must be satisfied. The autopilot structure contains the compensator *G(s)*, without the prefilter *F(s)*. The autopilot is a *series-type PID* controller, which assures zero stationary error for step type signal on both reference and perturbation inputs.

The optimal bounds are illustrated in Fig. 21.

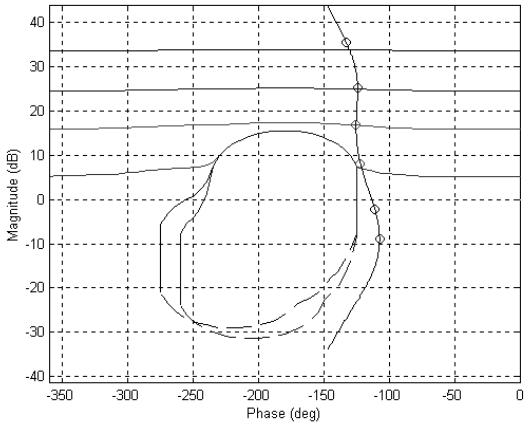

Fig. 21. Optimal bounds and nominal loop transmission for course-keeping autopilot

The nominal loop transmission is calculated for the same extended frequency vector, with w_1 values marked distinctly.

The bounds of robust stability and input disturbance rejection are determined on the basis of the performance specifications, ship templates and nominal ship model, which are computed in the same manner.

For disturbance rejection specifications, the maximum value α_P has been decreased:

$$\alpha_P = 0.03 = -30.5 \text{ dB}.$$

The disturbance rejection bounds are higher in this case, which implies bigger values for autopilot gains.

Again, the compensator is a *series-type PID* controller of the general form given in (27) and its structure is determined up-front.

Modifying the compensator expression, the nominal loop transmission is synthesized to satisfy the optimal bounds, without penetrating the closed contours, as shown in Fig. 21.

The final expression of the compensator is:

$$G(s) = -\frac{945s^2 + 233s + 3}{s^2 + 6.6s} =$$

$$= \frac{-945 \cdot (s + 0.2329) \cdot (s + 0.01363)}{s \cdot (s + 6.6)} \qquad (32)$$

The parameter values are: $T_I = 73.4$, $T_D = 4.3$, $T_P = 0.1515$ and $k_R = -33.35$ (33)

It can be observed that the gain value is bigger and the time constants are smaller.

The frequency characteristics of autopilot are illustrated in Fig. 22.

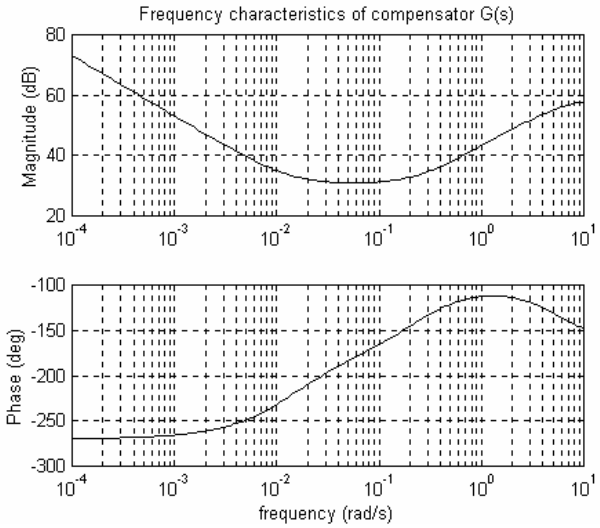

Fig. 22. Frequency characteristics of course-keeping autopilot

The closed loop system verifies the robust stability specification, as shown in Fig. 23.

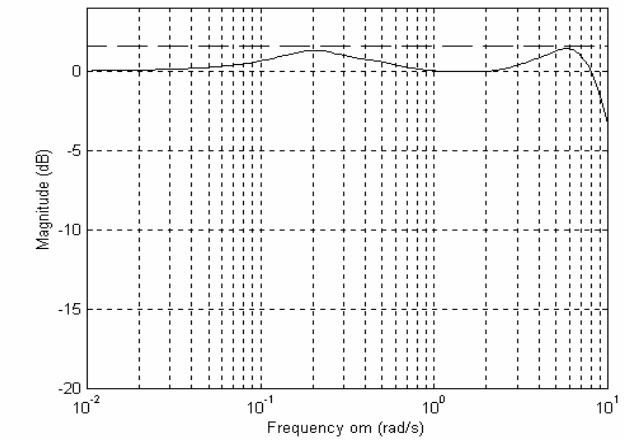

Fig. 23. Robust stability verification for course-keeping autopilot

The maximum magnitude characteristic envelope is smaller than the specified value for the entire working bandwidth:

$$\max_{H_{\delta\psi}(s),\,\omega}\left(\left|H_B(j\omega)\right|\right)=1.1823 < \alpha_B=1.2 \qquad (34)$$

Also, the disturbance rejection condition is satisfied, as illustrated in Fig. 24.

The maximum admissible value of input disturbance rejection $\alpha_P = 0.03 = -30.5$ dB is represented with dashed line.

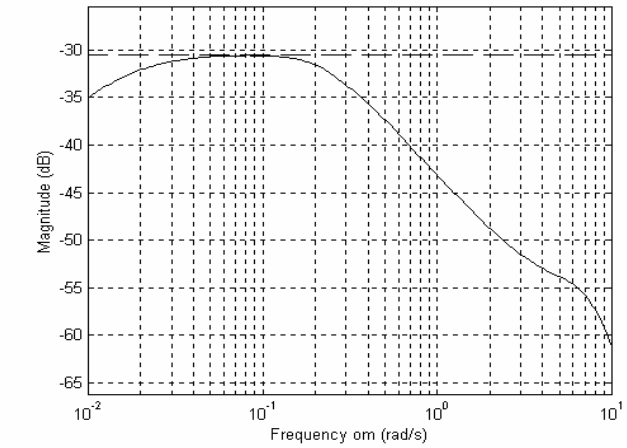

Fig. 24. Disturbance rejection verification for course-keeping autopilot

The magnitude characteristic envelope of the perturbation channel is smaller than the specified value:

$$\max_{H_{\delta\psi}(s),\,\omega}\left(\left|H_P(j\omega)\right|\right)=0.0296 < \alpha_P=0.03 \qquad (35)$$

The reference step responses of the closed loop system for all the ship models considered on the contour of the uncertainty region (N=20) are illustrated in Fig. 25. Depending on the ship model, the PID effect is different.

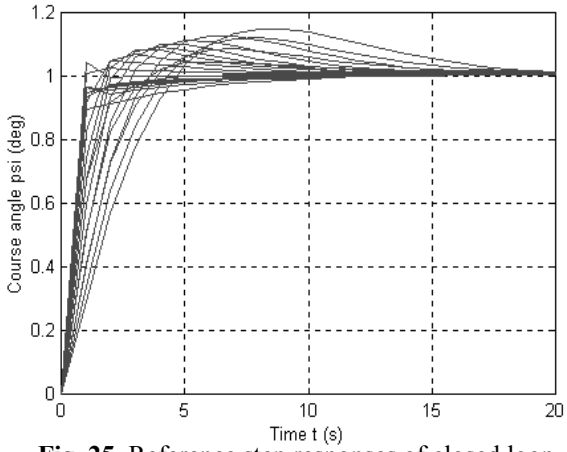

Fig. 25. Reference step responses of closed loop system for course-keeping autopilot

Using the same wave disturbances and ship model, the course-keeping effect using QFT autopilot is illustrated in Fig. 26. The waves have the significant height $h_{1/3} = 4$ *m* and the incidence angle $\gamma = 135$ *deg*. The parameters of the ship model correspond to the ship's forward speed $u = 22$ *Knots*, which was chosen on the upper limit of the speed range.

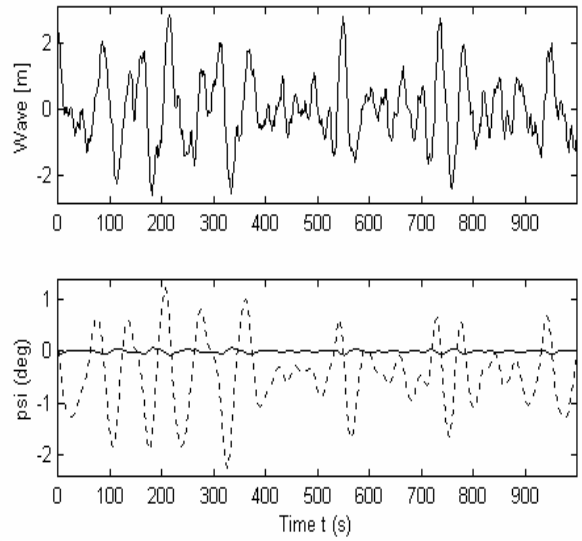

Fig. 26. Course stabilization with QFT autopilot

In the first figure, the wave disturbance corrected with incidence angle is illustrated. Due to incidence angle, the wave spectrum is moved to higher frequencies, changing the disturbance characteristics. As a result, the wave has smaller amplitudes and higher frequency components.
In the second figure, yaw angles are represented in two situations: without using QFT autopilot (drawn with dotted line) and with autopilot (continuous line). The reduction effect of yaw angle is obviously.

6. CONCLUSIONS

Robust QFT ship autopilot is designed, for the course-changing and course-keeping control of a ship. The ship model is affected by wave disturbances and has parametric uncertainties due to the forward speed, which affects hydrodynamic coefficients. Knowing the variation ranges of the model parameters, QFT autopilot can be design to satisfy performance specifications. The autopilot satisfies the robust stability, tracking performance and disturbance rejection conditions, for all ship models generated by the uncertainty region.

REFERENCES

[1] T. I. Fossen, Guidance and Control of Ocean Vehicles, John Wiley and Sons, New York, 1994.

[2] J. Van Amerongen, "Adaptive Steering of Ships – A Model Reference Approach", Automatica, vol. 20, no. 1, pp. 3-14, 1984.

[3] M. Blanke and M. Knudsen, "A sensitivity approach to identification of ship dynamics from sea trial data", Proc. of the IFAC Conf. CAMS'98, Fukuoka, pp. 261-269, 1998.

[4] K. Nomoto, T. Taguchi, K. Honda and S. Hirano, "On the Steering Qualities of Ships", Technical Report, International Shipbuilding Progress, vol. 4, 1957.

[5] N. H. Norrbin, "On the Design and Analyses of the Zig-Zag Test on Base of Quasi-Linear Frequency Response", Tech. Report B104-3, Swedish State Shipbuilding Experimental Tank (SSPA), Gothenburg, Sweden, 1963.

[6] M. J. Dove and C. B. Wright, "Development of marine autopilots", Computer methods in marine and offshore eng., pp.259-272, 1991.

[7] C. Yang, P. C. Austin and C. M. Xiao, "An H-inf controller with feedforward for yacht course-keeping", in Proc. of the IFAC Conf. CAMS 2001, Glasgow, Scotland,UK, 2001.

[8] N. A. Fairbaim and M. J. Grimble, "H-inf Marine Autopilot Design for Course-Keeping and Course-Changing", in Proc. of SCSS'90, pp. 3311-3335, Bethesda, MD, 1990.

[9] D. Popescu, Analiza si sinteza sistemelor robuste, Editura Universitaria, Craiova, 2002.

[10] J. C. Wu, A. K. Agraval and J. N. Yang, "Application of Sliding Mode Control to a Benchmark Problem", in Proc. of the ASCE Structures Congress, Portland, 1997.

[11] T. M. R. Rueda, F. J. G. Velasco, E. P. Moyano and E. G. Lopez, "Robust QFT controller for marine course-changing control", 5th Int. Symposium on Quantitative Feedback Theory and Robust Frequency Domain Methods, Public University of Navare, Pamplona, Spain, 2001.

[12] C. H. Houpis and S. J. Rasmussen, Quantitative Feedback Theory. Fundamentals and Applic., Marcel Dekker Inc., New York, 1999.

[13] M. B. McFarland and A. J. Calise, "Robust Adaptive Control of Uncertain Nonlinear Systems Using Neural Networks", in Proceedings of the American Control Conf., Albuquerque, New Mexico, 1997.

[14] S. Rumyantzev, A. Miroshnikov and E. Popova, "Design of PID controllers for ship course-keeping using approximations to H-inf solutions", in Proc. of IFAC Conference CAMS 2001, Glasgow, UK, 2001.

[15] V. Nicolau and E. Ceangă, "Wave spectrum correction with the ship's speed and the incidence angle", in Proc. of IFAC Conference CAMS 2001, pp. 331-336, Glasgow, UK, 2001.

[16] V. Nicolau, E. Ceangă, R. Popa and D. Aiordachioaie, "Robust ship autopilot for course-keeping and course-changing control using QFT method", in Proc. of the 6th IEEE Int. Conf. on Technical Informatics (CONTI 2004), Scientific Bulletin of "Politehnica" Univ. of Timişoara, Vol. **49** (63), No.1, pp. 67-72, Timişoara ISSN 1224-600X.

[17] M. A. Abkowitz, Lectures on Ship Hydrodynamics – Steering and Manoeuvrability, Tech. Report, nr. Hy-5, Hydro- and Aero-dynamics Laboratory, Lyngby, Denmark, 1964.

[18] P. G. M. Van der Klugt, "Rudder Roll Stabilization", Ph.D. Thesis, Delft University of Technology, 1987.

[19] C. G. Kallstrom, "Identification and Adaptive Control Applied to Ship Steering", Ph.D. Thesis, Lund Institute of Tech., Lund, Sweden, 1979.

[20] V. Nicolau, "Contribuții privind conducerea automată avansată a sistemelor navale", Ph.D. Thesis, Universitatea "Dunărea de Jos" Galați, Galați, 2004.